Progress In Electromagnetics Research Letters, Vol. 39, 37–47, 2013

A COMPARISON OF ULTRA WIDE BAND CONVENTIONAL AND DIRECT DETECTION RADAR FOR CONCEALED HUMAN CARRIED EXPLOSIVES DETECTION

Stuart W. Harmer*, Nicholas J. Bowring, Nacer D. Rezgui, and David Andrews

Sensing and Imaging Group, Manchester Metropolitan University, UK

Abstract—This paper describes how information about the electromagnetic structure of targets can be obtained from direct detection radar techniques, where the relative phase of the transmitted and received signals is not measured. A comparison is made between the resolved structure of a simple test target from an ultra wide band, pulse synthesis direct detection radar system at 14–40 GHz and an equivalent heterodyne radar receiver where phase information is recorded. The test targets employed are wax sheet of thickness 20 mm and 80 mm which are illuminated alone and in contact with the human body. A vector network analyser is used as the radar system. The simplicity of constructing ultra wide band direct detection radar systems combined with their cost makes the use of such radar systems appealing for applications such as concealed threat detection and non-destructive testing, where absolute range to the target, if required, can be determined by other methods.

1. INTRODUCTION

Ranging to scattering targets is a pre-requisite of RADAR (RAdio Detection And Ranging) systems [1]. The range information results from the round trip time of the transmitted electromagnetic signal, which may be a pulse in the time domain or a wide band emission in the frequency domain to synthesise such as pulse [2]. Additional information, about the internal shape and structure of the target may also be obtained if the temporal resolution of the radar is sufficient

Received 25 January 2013, Accepted 8 March 2013, Scheduled 8 April 2013

* Corresponding author: Stuart William Harmer (s.harmer@mmu.ac.uk).

to allow such details to be discriminated from the overall scattered signal [3]. Applications such as non destructive testing and concealed weapons detection require excellent range resolution in order to give capability to discern objects that are in close proximity [4, 5].

In frequency modulated radar systems the received signal has both amplitude, determined by the roundtrip distance travelled by the signal and the radar cross section of the scattering object, and phase, determined by signal frequency, roundtrip distance and the nature of the scattering object. Recovery of the phase of the received signal, with reference to the emitted signal, is a key process in radar receiver designs and permits ranging to the scattering body as described below in (1) and (2). In direct detection radar, the received signal phase is not measured as there is no mixing of the received signal with the transmitted, thus the range to the scattering object is not determined; however thin film effects from interference within a transparent target object, for example a low loss sheet of dielectric material, provide information on the structure (thickness and dielectric constant) of the object. In direct detection UWB radar, the transmitted pulse is swept, linearly with time, over its operating frequency range. The received, reflected, pulse is synchronised to that transmitted by *a-priori* knowledge of the sweep time, allowing the appropriate frequency channels to be allocated. Ranging to the target is usually required to scale the received signal, depending on where the signal was reflected from, and this ranging can be accomplished by much narrower band homodyne radar as the range to target is generally not required at the same resolution as is desired for target structure. The authors have previously used just such systems to detect the presence of explosives concealed on the human body [6–14]. The advantage of such an approach is primarily one of cost and simplicity, for example UWB band radar can be built using a direct detection MMIC which was intended for use as broad band passive microwave imager.

2. THEORETICAL DISCUSSION

Assuming a mono-static radar system, where the transmitter and receiver are co-located and also that the wavefront of the electromagnetic waves illuminating the target are approximately planar, i.e., the target is in the far field, then the received signal in the frequency domain can be written as:

$$S(\nu) = A(\nu)\Gamma(\nu)\exp\left(-i\frac{4\pi\nu}{c}z_0\right) \tag{1}$$

And in the time domain as,

$$s(t) = \Im^{-1}\left\{A(\nu)\Gamma(\nu)\exp\left(-i\frac{4\pi\nu}{c}z_0\right)\right\} \tag{2}$$

where ν is the frequency in cycles per second, c the speed of light, and $\Im^{-1}$ the inverse Fourier transform operation. The range to the target, z_0, is encoded in the phase of the propagation term; the transmitter and receiver antenna frequency response is A, and the structure of the target is encoded in the reflectivity term Γ. Invoking the convolution theorem we can write (2) as a temporal convolution of the amplitude, reflection and roundtrip terms:

$$s(t) = \frac{1}{2\pi}\Im^{-1}\{A(\nu)\} \otimes \Im^{-1}\{\Gamma(\nu)\} \otimes \delta\left(t - \frac{2z_0}{c}\right) \tag{3}$$

Here we use the symbol $\otimes$ to represent the convolution operation. The reflection term from (3) reveals information on the structure of the target. For example: a wax layer, in air, which is highly transparent to electromagnetic radiation at microwave frequencies [15], has a reflectivity at normal incidence which can be described by [16],

$$\Gamma(\nu) = \frac{\Gamma_{wax}\left(1 - \exp\left(i2\kappa h\right)\right)}{1 - \Gamma_{wax}^2\exp\left(i2\kappa h\right)} \tag{4}$$

where, $\Gamma_{wax} = \frac{1-\sqrt{\varepsilon_{wax}}}{1+\sqrt{\varepsilon_{wax}}}$, the thickness of the wax layer is h, and the value of ε_{wax} over the microwave frequency range, 14–40 GHz, is approximately constant with real part of permittivity of 2.20 (refractive index 1.48), with a loss tangent of $< 3 \times 10^{-4}$ [15]. (4) maybe written as an infinite sum of terms [7]; taking only the principal reflections from the first (air/dielectric) and second (dielectric/air) interfaces,

$$\Gamma = \Gamma_{wax}\left(1 - \left(1 - \Gamma_{wax}^2\right)\exp\left(i2\kappa h\right)\right) \tag{5}$$

where, $\kappa = \frac{2\pi\nu}{c}\sqrt{\varepsilon_{wax}}$; the imaginary part of κ can be neglected as it is much smaller than the real part by virtue of the extremely low loss nature of wax at microwave frequencies.

Application of (3) to (5) gives the time domain signal reflected from the wax block,

$$\begin{aligned} s(t) \;=\; & \Gamma_{wax}\Im^{-1}\{A(\nu)\} \otimes \ldots \left(\delta\left(t - \frac{2z_0}{c}\right)\right. \\ & \left. - \left(1 - \Gamma_{wax}^2\right)\delta\left(t - \frac{2}{c}\left(z_0 + \sqrt{\varepsilon_{wax}}h\right)\right)\right) \end{aligned} \tag{6}$$

The effect of the transmitter and receiver response, A can be removed by an appropriate deconvolution with a calibration signal,

for example the reflection from a metal plate [17], giving,

$$s(t) = \Gamma_{wax} \ldots \left(\delta \left(t - \frac{2z_0}{c} \right) - \left(1 - \Gamma_{wax}^2\right) \delta \left(t - \frac{2}{c} \left(z_0 + \sqrt{\varepsilon_{wax}} h \right) \right) \right) \quad (7)$$

A similar equation can be derived for the case of a wax layer positioned on the human body, mimicking a layer of explosive material [7],

$$s(t) = \Gamma_{wax} \delta \left(t - \frac{2z_0}{c} \right) + \ldots \Gamma_{body} \left(1 - \Gamma_{wax}^2\right) \delta \left(t - \frac{2}{c} \left(z_0 + \sqrt{\varepsilon_{wax}} h \right) \right) \quad (8)$$

where, $\Gamma_{body} = \frac{\sqrt{\varepsilon_{wax}} - \sqrt{\varepsilon_{body}}}{\sqrt{\varepsilon_{wax}} + \sqrt{\varepsilon_{body}}}$, and ε_{body} is the complex permittivity of the human body, which is frequency dependent and well approximated by [18].

The general relationship between the phase sensitive time domain signal $s(t)$ and the power detection counterpart, $s'(\tau)$, is given by,

$$s'(\tau) = \frac{1}{2\pi} s^*(-t) \otimes s(t) \quad (9)$$

which is equivalent to taking the inverse Fourier Transform of the power spectrum of the signal $|S(\nu)|^2$. Here we have used the letter τ to denote time in the direct detection case. Applying (9) to (7) and (8), gives the analogous direct detection signal expected from the wax in air and the wax on body respectively,

$$\begin{aligned} s'_{wax}(\tau) \;=\; & |\Gamma_{wax}|^2 \left(\left(1 + \left| \left(1 - \Gamma_{wax}^2\right) \right|^2 \right) \delta(\tau) \ldots \right. \\ & \left. -2\mathrm{Re} \left\{ \left(1 - \Gamma_{wax}^2\right) \right\} \delta \left(\tau - \frac{2\sqrt{\varepsilon_{wax}} h}{c} \right) \right) \end{aligned} \quad (10)$$

and,

$$\begin{aligned} s'_{body}(\tau) \;=\; & \left(|\Gamma_{wax}|^2 + \left| \Gamma_{body} \left(1 - \Gamma_{wax}^2\right) \right|^2 \right) \delta(\tau) + \ldots \\ & 2\mathrm{Re} \left\{ \Gamma_{wax}^* \Gamma_{body} \left(1 - \Gamma_{wax}^2\right) \right\} \delta \left(\tau - \frac{2\sqrt{\varepsilon_{wax}} h}{c} \right) \end{aligned} \quad (11)$$

The simple conversion between time and optical path length (in vacuum) is given by the relationship, $z = \frac{ct}{2}$ for the case in conventional radar signals and $z = \frac{c\tau}{2}$ for the depth in direct detection radar signals. Comparison of (7) and (8) with (10) and (11) show that direct detection radar reveals the characteristic optical spacing of the interfaces, $\sqrt{\varepsilon_{wax}} h$, but not the range z_0 to the target. The amplitudes, reflected by each interface are also different between conventional and direct detection radar; the strength of reflections from the two interfaces are mixed or combined in the direct detection case and are

not separable. However it is clear that information about the spacing between the interfaces and the reflectance of the target may still be obtained with a direct detection approach. The signals predicted by (10) and (11) have been evaluated for an 80 mm thick wax sheet for a bandwidth of 25 GHz (15–40 GHz range), see Figure 1.

Higher order terms in (4) result in smaller amplitude reflections at integer multiples of the optical thickness of the slab, i.e., at $n\sqrt{\varepsilon_{wax}}h$, where $n = 2, 3, 4, \ldots$. In practice these reflections are generally much smaller than the two principal reflections discussed, and cannot usually be resolved easily experimentally.

A critical figure of merit for UWB direct detection radar is the range resolution of the system, this is given by,

$$\Delta z \geq \frac{c}{2 \times \sqrt{\varepsilon} BW} \tag{12}$$

where BW is the frequency range over which the radar is sensitive, and ε is the permittivity of the layer. In the case considered the best resolution that can be expected is about 4 mm.

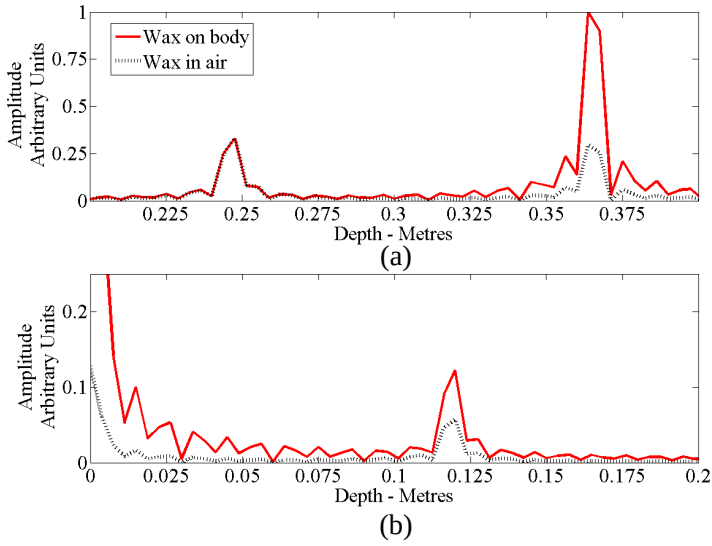

Figure 1. Graphical display of the predicted reflected signal from an 80 mm thick wax sheet in air and in contact with the human body, the sheet is 250 mm from the radar. 1024 frequency data points are used and the radar operates over 15–40 GHz. Both the (a) conventional radar signal and (b) direct detection radar depict the reflection from the two interfaces of the wax sheet $\sim$ 120 mm apart due to the optical depth of the sheet.

3. MEASURED RESULTS

Experimental results, to demonstrate similarities and differences between conventional and direct detection, were taken with an Agilent E8363B vector network analyser with waveguide horns attached to ports 1 and 2. Both horns were pointed at the target and the complex

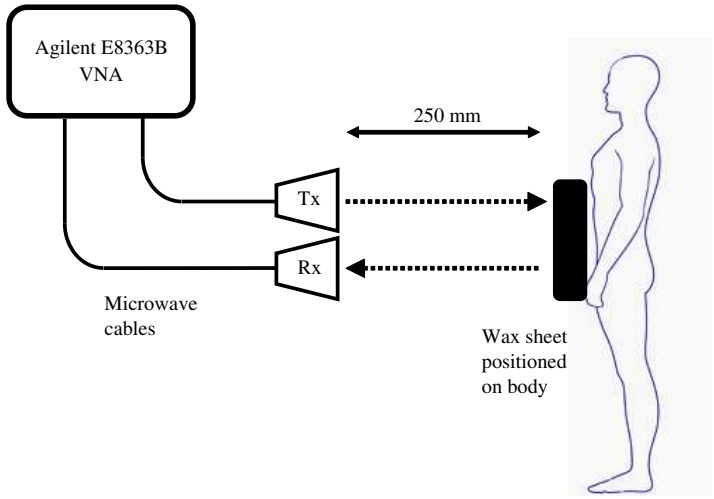

Figure 2. An illustration of the experimental apparatus used to obtain depth spectra from wax sheets positioned in contact with the human body.

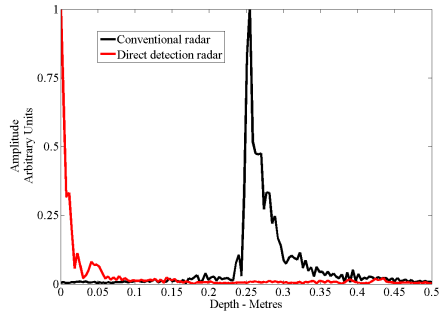

Figure 3. A graphical comparison of conventional and direct detection radar data for a clothed human torso without additional dielectric layers present; there is one obvious peak in both plots that corresponds to the reflection form the body.

reflected field was recorded as S_{21} at 1024 equally spaced frequencies over the band 15–40 GHz. The wax sheets, both on person and off person, were situated ~ 250 mm from the horn antennae, see Figure 2. The signals were transformed to the time domain using an Inverse fast Fourier Transform (IFFT) implemented in Matlab, and the amplitude of the reflected signal presented as a function of range, see Figures 3–7. The time delay associated with propagation in the cables that connect the horn antennae to the VNA have been subtracted for these plots. To simulate a direct detection radar the S_{21} signal was multiplied by its complex conjugate prior to the IFFT to give a depth spectrum.

The reflected signal from a stationary human torso consists of a simple peak in the conventional radar plot, see Figure 3, and the relatively constant frequency response of the direct detection signal gives a single zero frequency (DC) peak. By comparison the signal from an isolated, 80 mm thick, wax block, see Figure 4, shows two distinct peaks separated by 120 mm in range and the direct detection plot has an additional peak at the same distance, 120 mm. When the wax block is attached to the front of the torso, a similar pattern is observed, see Figure 5, though the reflection from the torso is generally greater than

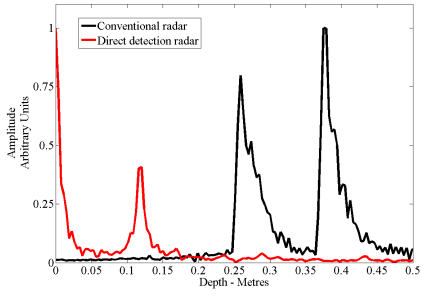

Figure 4. A graphical comparison of conventional and direct detection radar data for a 80 mm thick wax sheet in air; there are clearly two peaks in both plots that correspond to the reflections form the front and back interfaces of the wax sheet. The optical depth is about 120 mm, corresponding to a refractive index of ~ 1.5 (permittivity of 2.25).

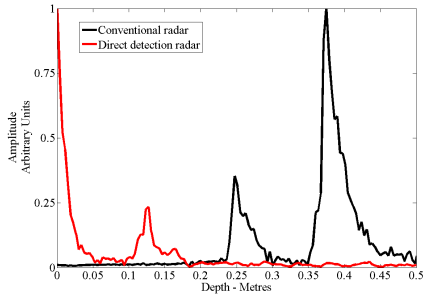

Figure 5. A graphical comparison of conventional and direct detection radar data for a clothed human torso with the 80 mm thick wax sheet in contact with the human torso; the two peaks in both sets of radar data are associated with the reflections from the air/wax interface and the wax/body interface. Contrast with Figure 2 for the body without wax layer.

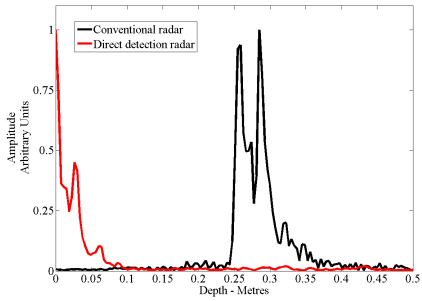

Figure 6. A graphical comparison of conventional and direct detection radar data for a much thinner, 20 mm thick, wax sheet in air; again there are clearly two peaks in both plots that correspond to the reflections form the front and back interfaces of the wax sheet. The optical depth is about 30 mm, corresponding to a refractive index of ~ 1.5 (permittivity of 2.25).

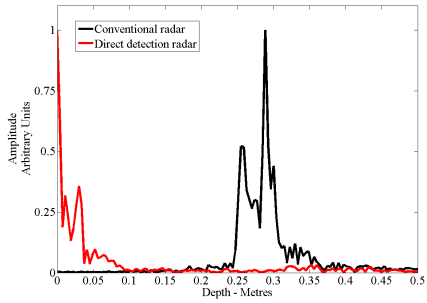

Figure 7. A graphical comparison of conventional and direct detection radar data for a clothed human torso with the thinner, 20 mm thick, wax sheet in contact with the human torso; the two peaks in both sets of radar data are associated with the reflections from the air/wax interface and the wax/body interface.

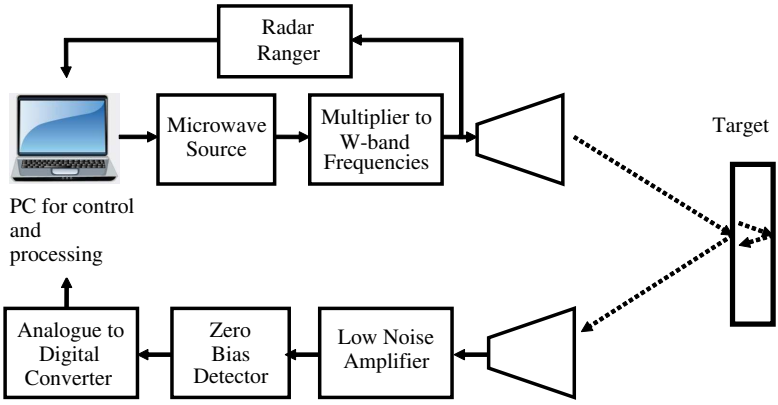

Figure 8. The block diagram of a direct detection radar of the type used by the authors for the detection of simulated explosive layers at stand-off distances [14].

that from the wax/air interface due to the greater difference in the permittivity of wax and body when compared to wax and air. Further results are presented in Figures 6 and 7, where a, thinner, 20 mm thick

wax sheet is used. The peaks are close together ($\sim 30\,\text{mm}$), but still easily resolved.

It may be noted that the peaks in the direct detection plot are generally sharper and better defined than the corresponding conventional radar peaks. The data shown has not been corrected for the electromagnetic response of the antennae, which contribute to the observed signal as described in (1) and (3) and leads to a broadening or 'tail' to the range response. Direct detection however is not sensitive to the phase, but only to the square of the complex amplitude and therefore the broadening effect is reduced because the width of the temporal antennae response is shortened.

4. SUMMARY

Direct detection radar systems can be used to determine the internal structure of semi-transparent materials, such as dielectric layers. These layers can be positioned on the human body to simulate the effect of a human carried explosive device consisting of plastic explosive material such as RDX or PETN. Only explosive materials which have low dielectric loss can be detected by the interferometric technique outlined. Explosive materials containing absorbed water, for example ammonium nitrate, will result in high attenuation of the wave reflected from the body and consequently there will be no second peak as is seen with the wax sheets.

Unlike conventional radar systems, where relative phase and amplitude are recorded, direct detection radar systems only record the power (square of amplitude). Ultra wide band radar systems can be simply constructed using the direct detection approach as there is no need for intermediate frequency stages that are employed in conventional heterodyne radar systems. Another significant advantage is cost; expensive components such as mixers are not required and the radar receiver can be realised from a single MMIC type receiver. This is particularly important for higher frequency band radar (i.e., millimetre wave and above), where transmitters typically use multipliers and sub harmonic detection.

It is also seen that the effect of antenna response is reduced due to the phase independent measurement technique, giving sharper features in the time or depth domains, see Figure 5 for example. Another favourable feature of direct detection radar is the immunity of the signal to target movement, this a result of the phase insensitivity of the system. Two significant disadvantages of a direct detection approach are the inability of such systems to determine absolute range to the scattering object and the lack of clutter rejection that is inherent

due to the absence of phase information. The authors have, however, overcome the ranging problem by generating two alternating frequency sweeps for transmission. An UWB sweep is used for the direct detection radar for determination of object structure as outline in this paper, and a much narrower frequency sweep is used for homodyne ranging. Clutter rejection with direct detection radar by range gating is not possible as the amplitude terms from each reflection are combined together, see (10) and (11), making the range gating of reflecting surfaces of interest impossible as is clearly seen in Figures 3–7.

The results demonstrate that there is potential for direct detection radar to be applied for the remote detection of concealed objects and especially of concealed explosive devices as the radar can be made compact and can provide the high resolution required to discriminate the presence of objects placed in front of the body.

The authors have employed an UWB direct detection radar of the type outlined in Figure 8 to realise stand-off range, ~ 35 metres, remote sensing for concealed explosives and weapons by making use of the interference techniques discussed in the in conjunction with polarimetry [14].

REFERENCES

1. Levanon, N., *Radar Principles*, 1–2, John Wiley & Sons, New York, 1988.
2. Robinson, L. A., W. B. Weir, and L. Young, "An RF time-domain reflectometer not in real time," *IEEE Trans. Microwave Theory Tech.*, Vol. 20, 855–857, Dec. 1972.
3. Park, J. S. and C. Nguyen, "A new millimeter-wave step-frequency radar sensor for distance measurement," *IEEE Microwave Wireless Compon. Lett.*, Vol. 12, No. 6, 221–222, Jun. 2002.
4. Boryssenko, A., O. Boryssenko, A. Lishchenko, and V. Prokhorenko, "Inspection of internal structure of walls by subsurface radar," *IEEE Aerosp. Electron. Syst. Mag.*, Vol. 21, No. 10, 28–31, Oct. 2006.
5. Sheen, D., D. McMakin, and T. E. Hall, "Three-dimensional millimeter-wave imaging for concealed weapon detection," *IEEE Trans. Microwave Theory Tech.*, Vol. 49, No. 9, 1581–1592, 2001.
6. Andrews, D. A., S. E. Smith, N. D. Rezgui, N. J. Bowring, M. Southgate, and S. W. Harmer, "A swept millimetre-wave technique for the detection of concealed weapons and thin layers of dielectric material with or without fragmentation," *Proc. SPIE*, Vol. 7309, 2009.

7. Andrews, D. A., N. Rezgui, S. E. Smith, N. J. Bowring, M. Southgate, and J. G. Baker, "Detection of concealed explosives at standoff distances using wide band swept millimetre waves," *Proc. SPIE*, Vol. 7117, 2008.
8. Bowring, N. J., J. G. Baker, N. Rezgui, M. Southgate, and J. F. Alder, "Active millimetre wave detection of concealed layers of dielectric material," *Proc. SPIE*, Vol. 6540, 2007.
9. Agurto, A., Y. Li, G. Y. Tian, N. Bowring, and S. Lockwood, "A review of concealed weapon detection and research on perspective," *Proc. IEEE ICNSC*, 443–448, 2007.
10. Bowring, N., D. Andrews, N. D. Rezgui, and S. W. Harmer, "Remote detection and measurement of objects," U.K. Patent 2 458 764, Mar. 18, 2009.
11. Andrews, D. A., N. J. Bowring, N. D. Rezgui, M. Southgate, E. Guest, S. W. Harmer, and A. Atiah, "A multifaceted active swept millimetre-wave approach to the detection of concealed weapons," *Proc. SPIE*, Vol. 7117, 2008.
12. Bowring, N. J., J. G. Baker, N. D. Rezgui, and J. F. Alder, "A sensor for the detection and measurement of thin dielectric layers using reflection of frequency scanned millimetric waves," *Meas. Sci. Technol.*, Vol. 19, No. 2, 024004, Jan. 2008.
13. Bowring, N. J., J. G. Baker, and J. F. Alder, "Detection and measurement of thin dielectric layers using reflection of scanned millimetric waves," *Proceedings of the IEEE International Conference on Networking, Sensing and Control*, 437–442, Apr. 2007.
14. Harmer, S. W., N. J. Bowring, D. Andrews, and N. D. Rezgui, "A review of nonimaging stand-off concealed threat detection with millimeter-wave radar," *IEEE Microwave Magazine*, Vol. 13, No. 1, 160–167, Jan.–Feb. 2012.
15. Lamb, J. W., "Miscellaneous data on materials for millimetre and submillimetre optics," *Int. J. Infrared Millim. Waves*, Vol. 17, No. 12, 1997–2034, 1996.
16. Harmer, S. W., P. D. Townsend, and N. J. Bowring, "Enhancement of photomultiplier sensitivity with anti-reflective layers," *J. Phys. D: Appl. Phys.*, Vol. 45, No. 5, 055102, Feb. 2012.
17. Gashinova, M., V. Djigan, L. Y. Daniel, and M. Cherniakov, "Adaptive calibration in UWB radar," *Proc. IEEE Radar Conference*, 1161–1166, May 2008.
18. Buchner, R., G. T. Hefter, and P. M. May, "Dielectric relaxation of aqueous NaCl solutions," *J. Phys. Chem. A*, Vol. 103, No. 1, 1–9, Dec. 1998.